

# **The impact of neighborhood layout heterogeneity on carbon emissions in high-density urban areas: A case study of New Development Areas in Hong Kong**

Ping He <sup>a</sup>, Jin Xue <sup>a</sup>, Geoffrey Qiping Shen <sup>a, \*</sup>, Meng Ni <sup>a</sup>, Shengwei Wang <sup>b</sup>, Han Wang <sup>a</sup>,  
Lijie Huang <sup>a</sup>

<sup>a</sup> Department of Building and Real Estate, The Hong Kong Polytechnic University,  
Kowloon 999077, Hong Kong, PR China

<sup>b</sup> Department of Building Environment and Energy Engineering, The Hong Kong  
Polytechnic University, Kowloon 999077, Hong Kong, PR China

\*Corresponding author

E-mail address: bsqpshen@polyu.edu.hk

## **Abstract**

Under the climate change context, there is a universal appeal for a paradigm shift towards environmentally sensitive urban design. Previous studies focused on density parameters, while ignoring the rational layout of buildings in the neighborhood, especially the layout heterogeneity, which would cause different environmental performance outcomes under the intricate and dynamic interdependence among buildings. This study systematically explores the impact of five neighborhood layout heterogeneity indicators, including the coefficient of variation of building height, footprint area, volume, footprint aspect ratio, and surface-to-volume ratio, on carbon emissions, with consideration of several scenarios regarding different renewable energy application ratios. Totally 384 neighborhood cases

are modeled under the same planning conditions in a new development area in Hong Kong and examined with the same simulation assumptions so as to exclude the impact of non-design related factors. The joint influences of different neighborhood layout indicators are examined by multiple linear regression analysis. The statistical results confirm the significant impacts of heterogeneity of building density and shape on neighborhood carbon emissions. It is found that the heterogeneity of building height would impede carbon reduction efforts due to higher mutual shading on rooftops and thus less solar harvesting, while the carbon reduction by building façade solar energy collection could be improved by the heterogeneity of building shape, including the variation of aspect ratio and surface-to-volume ratio. When considering both energy consumption and renewable energy collection, the heterogeneity of building height can lead to less net carbon emissions while that of building shape results in more net carbon emissions. Notably, the heterogeneity of neighborhood layout design would lead to the opposite result in carbon reduction efforts regarding solar energy collection and building energy consumption, which leaves a trade-off in decision-making when designing low-carbon neighborhoods.

## **Keywords**

Urban form; Urban morphology; Sustainable neighborhood; Spatial heterogeneity; Carbon emissions; Solar energy

## **1 Introduction**

Facing the challenge of climate change on human survival and development, reducing CO<sub>2</sub> emissions has been the focus of global efforts toward sustainable

development, especially in cities where more than half of the world's population now resides and they contribute around 70% of global carbon emissions [1]. Under the pressure of achieving the carbon neutrality goals, new urban developments are required to be planned to minimize their carbon emissions by cutting energy use, depending more on renewable sources, and increasing the carbon sink for CO<sub>2</sub> sequestration. A fundamental shift of the urban design approach that affects the urban form is required. In order to put this paradigm shift into effect, it is crucial to place more emphasis on the connection between the physical characteristics of new developments such as their structure, texture, volumes, and layout, and environmental performance [2].

In high-density urban areas, the neighborhood layout could affect more on the environmental performance compared with that in less compact areas, due to the dynamic and complex interconnection and interdependencies among buildings including the impact from shading, longwave radiant heat exchange, and solar reflection, as well as between the buildings and the urban environment such as building heat release to the ambient air, and urban heat island effect influences on building performance [3]. With the above mechanism, the neighborhood layout in the high-density area is assumed to be significantly related to carbon emissions. Firstly, as a result of the coupling effect and nearby microclimate warmed by heat emissions from buildings, the change of neighborhood layout can affect ventilation and then mitigate the urban heat island effect, which further influences the building heating or cooling demand and thus carbon emissions [4]. Secondly, in compact urban forms, the mutual shading among buildings can lead to different cooling and heating load and thus affect the carbon emission resulting from energy consumption [5, 6]. Moreover, in terms of the application of renewable energy generation such as solar energy

collecting, the availability of places for photovoltaic system installation and the level of obstruction, which are crucial factors in the reduction of carbon emissions, are sensitive to the mutual shading among buildings [7].

In order to have a better understanding of sustainable neighborhood design, previous studies have employed various spatial factors to look into the effect of neighborhood layout design on environmental performance, which can be classified into three groups. The first group explores the impact of building forms on neighborhood-scale environmental performance. These studies investigate the environmental influence of various kinds of archetypal building forms or special building shapes. For example, in order to examine the relationship between urban block typology, solar energy harvesting potential, and building energy use efficiency in the context of the tropical high-density city Singapore, Zhang, Xu [7] simulate thirty generic urban block cases across six typologies that represent a variety of urban forms. Hachem, Athienitis [8] reports the energy supply and demand of the buildings of rectangles and several variants of L shape with a straight or semi-circular arrangement. The second group focus on the relationship between site layout and environmental performance. Hachem-Vermette and Singh [9] investigate the solar energy exploitation capability of three neighborhood layout prototypes including a rectangular neighborhood, a circular layout, and a hexagonal-based layout. Hong and Lin [10] examine the impacts of building layouts and tree placement on the pedestrian-level outdoor wind environment and thermal comfort. These two groups emphasize and dig into macro or microscopes of neighborhood form and apply a qualitative way to differentiate different forms.

The third group probes into the urban form indicators. For instance, Salvati, Coch

[11] explore the effect of urban compactness measured by site coverage ratio on building energy performance including the urban heat island intensity and solar radiation availability in a Mediterranean climate. Mohajeri, Upadhyay [12] explore the relationship between various compactness indicators and solar potential in the 16 neighborhoods. Morganti, Salvati [13] explore the relationship of a set of urban morphology indicators on the building facade solar availability of 14 urban textures in the Mediterranean context. Chen, Wu [14] make comparisons of the impact of various building density and height at a fixed floor area ratio on block surface temperature. Alavipanah, Schreyer [4]’s and Hu, Dai [15]’s studies focus on the impact of height, footprint, and volume aspects of urban geometric indicators on urban thermal conditions. Ahmadian, Sodagar [16]’ and Xia and Li [17]’s studies explore urban developed types, density, and building energy performance interactions. These studies all focus on the overall density parameters, while ignoring the building distribution forms, such as spatial heterogeneity. With the planning techniques aiming to achieve higher constructed density without sacrificing the environmental quality of urban development [18], apart from the density parameter, reasonable spatial distribution and arrangement of buildings should be further discovered.

With the encouragement to break the monotonous development in urban design guidelines [19, 20], understanding the effects of spatial heterogeneity on the environment has garnered increasing attention. Spatial heterogeneity is defined either as the variation in space in the distribution of a point pattern, or the variation of a qualitative or quantitative value of a surface pattern [21]. Cheng, Steemers [22] firstly examine the horizontal and vertical urban layout randomness on solar potential, and affirm the importance of horizontal and vertical randomness design on neighborhood solar potential. Several studies

investigate the heterogeneity of building height on the solar energy capacity in local urban contexts [23-26]. Liao, Hong [27] examines the possible effects of geographical heterogeneity on surface urban heat islands. Street surface temperature and the average urban albedo are examined by Yang and Li [28] in relation to the effects of building density and building height heterogeneity. Shareef [29] examines the effects of urban morphology, particularly height variety, on the cooling load within regional climatic conditions of the United Arab Emirates.

Although the relationship between neighborhood layout and environmental performance has been explored from different perspectives in the above studies, and some of them dig into energy consumption and carbon emission performance, the exploration of spatial heterogeneity indicators focuses on building height diversity, while ignoring the building shape variation. They fail to systematically demonstrate the relationship between neighborhood layout heterogeneity and carbon emissions. Additionally, in previous work, the different planning and geometric parameters, which may affect each other, were examined independently, with their combined effects neglected.

To fill the research gap, we systematically investigate the impact of five neighborhood layout heterogeneity indicators, including the coefficient of variation of building height, footprint area, volume, footprint aspect ratio, and surface-to-volume ratio, on carbon emissions from buildings, with the exploration of the joint influence of the layout indicators by multiple regression analysis. A typical high-density new development area in Hong Kong is selected as study case and the local planning restrictions are referred to in this study for the neighborhood layout design. An easy-to-use GIS-based parametric workflow is applied to generate 3D neighborhood layout models for early-stage urban

design, and a validated software CitySim is use to assess the energy consumption and solar energy harvesting for carbon assessment. Then, a multiple regression model is applied to explore the impact of neighborhood layout heterogeneity on carbon emissions. The results provide guidelines for neighborhood design optimization in relation to the early-design process in dense urban areas. Besides, the study offers an effective and efficient GIS-based technique of analysis for the urban planning practitioners seeking applicable design solutions for minimizing carbon emissions and improve the local environmental performance.

## **2 Data and methodology**

Fig. 1 illustrates the flow chart of the methodology in this study. First, planning data of the case study area are collected, and then they are processed in the software CityEngine to generate hundreds of neighborhood cases with 3D building models. Geometric indicators and carbon emissions of each neighborhood are calculated. Finally, regression analysis is applied to explore the relationship between neighborhood layout heterogeneity and carbon emissions.

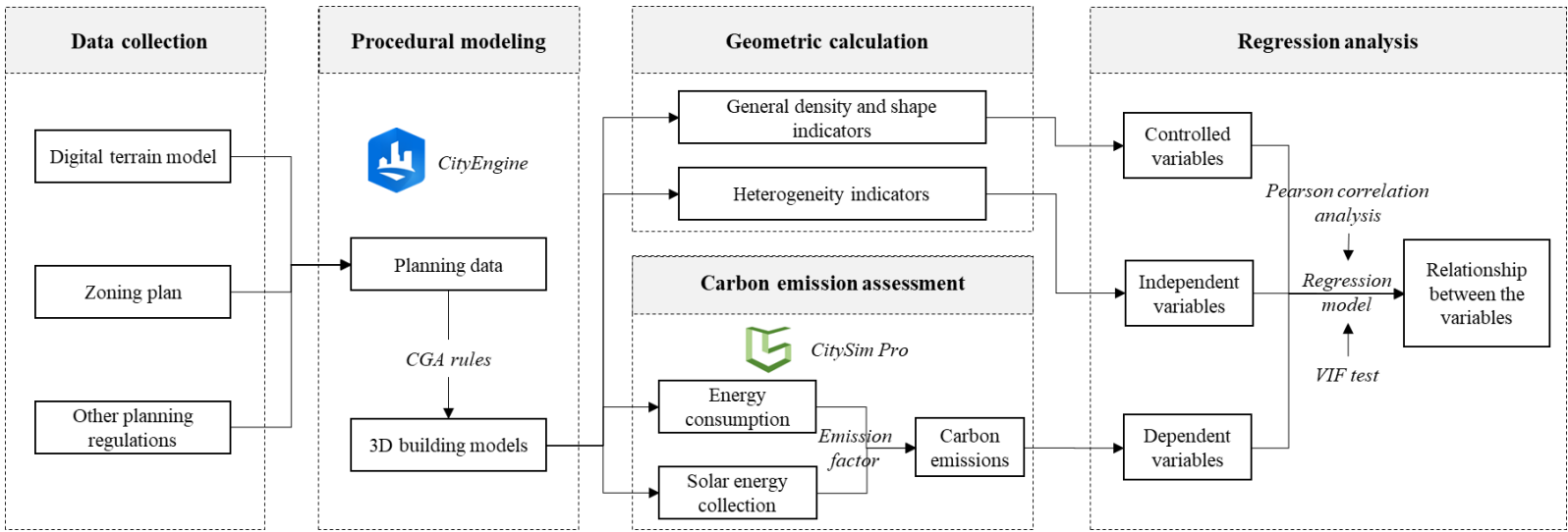


**Fig. 1.** Flowchart of the methodology

## 2.1 Study area

Kwu Tung North (KTN), located in the north part of Hong Kong (22.5078°N, 114.1002°E) (as shown in Fig. 2), is selected as the case study area in this research for the following three reasons. Firstly, KTN is a typical high-density neighborhood, which is suitable for the neighborhood layout design study as there are strong interconnections and interdependencies among buildings. Secondly, KTN is a typical new development neighborhood, the study of which would provide references for other new developments. It is one of the New Development Areas in Hong Kong, aiming at enhancing land supply, coping with the increase in population, and improving the living environment by decentralizing the population from the over-crowded urban districts. The planning scheme area of the KTN is about 447 ha and will accommodate a population of over 110,000 upon full development. Around 2/3 of the new housing units in the KTN are public houses, which is expected for high-density residential development. Thirdly, KTN is a typical pilot area for green planning. The local natural environment supports renewable energy adoption.



Located at the northern fringe of the tropical zone, the study area owns fruitful solar energy resources of an annual average global horizontal solar irradiance of 1,400 kWh/m<sup>2</sup> [30]. The potential PV power output in Hong Kong is at 5981GWh, which would account for 13.53% of the entire electricity consumption in 2020, cut imports of coal and natural gas by 25% and 54%, respectively, and prevent roughly 3 million tons of greenhouse gas emissions annually [31]. The local development strategy also supports the green planning of KTN. The Hong Kong government strives to build low-carbon liveable communities in the planned new development areas with initiatives that adopt green and sustainable design in buildings as far as possible to reduce energy consumption [32].

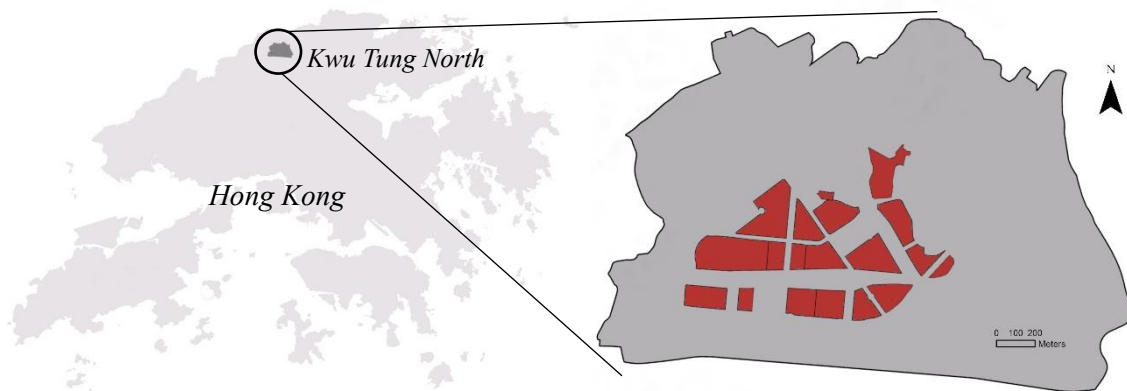


**Fig. 2.** Location of Kwu Tung North in Hong Kong (the residential areas are marked in red)

According to the planning documents, the residential areas are clustered in the center of the neighborhood, embraced by the commercial zone, government and community facilities area, and villages. The residential zones are intended for high-density residential developments. For simplicity, the buildings in the surrounding plots have not been taken into consideration for simulation in this study as the low-rise buildings have relatively little overshadowing of the residential buildings.

## 2.2 Procedural modeling

Semi-random neighborhood layouts and buildings are generated for carbon emission assessment. Pre-defined development restriction, which basically follows the codes and regulations in the planning documents enacted by the government, is applied to building generation, including maximum building site coverage, height and plot ratio. To simulate various forms of neighborhood layout, some randomness is added to zone subdivision, open space generation, and shape and volume of individual buildings. The modeling parameter settings and corresponding development restriction from the planning documents are described in Table 1. Several ranges of area are applied in the plot subdivision rules in order to simulate different degrees of heterogeneity. Referring the definition of high-rise building in Hong Kong (the buildings that exceed 30 m) and the height restriction in the planning area, the building height adopted in this study for 3D modeling is set between 30-110 m. As the site coverage restriction for high-rise domestic building should not exceed 37.5% for the given sites referring to Hong Kong Building Planning Regulations, and the site coverage should be approximate 15% when the height of buildings reaches the development restriction without breaking the plot ratio restriction, the site coverage adopted in this study is 15%-37.5%.

**Table 1.** 3D modeling parameter settings for the buildings

	Adopted in this study	Development restriction (upper limit) from the government documents
Plot subdivision rule	Recursive subdivision, Area ranges between: 3000-5000, 3000-7000, 3000-9000,	-

	5000-7000, 5000-9000, and 7000-9000 m <sup>2</sup>	
Site coverage	15%-37.5% randomly for each subplot	37.5% (Source: Building Planning Regulations)
Building height	30-110 m randomly for each subplot	110 m for high-density residential developments (Source: Outline Zoning Plan)
Plot ratio	≤6	5-6 for high-density residential developments (Source: Outline Zoning Plan)

210

211 ESRI CityEngine, a 3D modeling program based on procedural modeling and CGA  
 212 (Computer Generated Architecture) shape grammar principles, creates the 3D urban  
 213 environment. A group of semi-automatic procedures and approaches are used in procedural  
 214 modeling to create virtual environments and structures with less user intervention. Shape  
 215 rules are a collection of transformation rules, including spatial, boolean, and derivation  
 216 rules, that are applied to a base feature (such as points, lines, areas, and volumes) to produce  
 217 new shapes by sequentially moving from the general to the specific levels, assisted by the  
 218 composing attributes.

219 Geospatial data containing details on the positions, dimensions, and connections of  
 220 geographic elements are required for the creation of a 3D GIS model. Topographical maps,  
 221 which depict both natural and man-made features, are the primary source of this  
 222 information. The following are the data pieces needed for the current study:

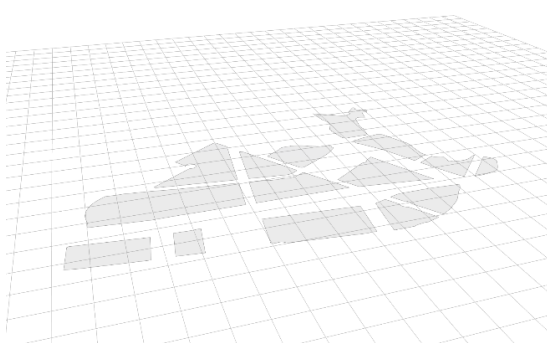
- 223 • Digital terrain model (DTM), constructed by interpolating the height points and  
 224 contour lines;
- 225 • Outline Zoning Plan (OZP) and Outline Development Plan (ODP), with land use  
 226 information and development restriction data of each plot in KTN;
- 227 • Other government planning documents, with additional development restriction

228 data.

229 These modeling components are crucial to the 3D method because they enable  
230 evaluation of the neighborhood's overall energy usage and production of renewable energy.  
231 As the research focuses on the general neighborhood layout, the building's interior structure  
232 has not been considered in the modeling. By modeling the general building's 3D shape, the  
233 spatial relationships between buildings and the urban context can be fully displayed.

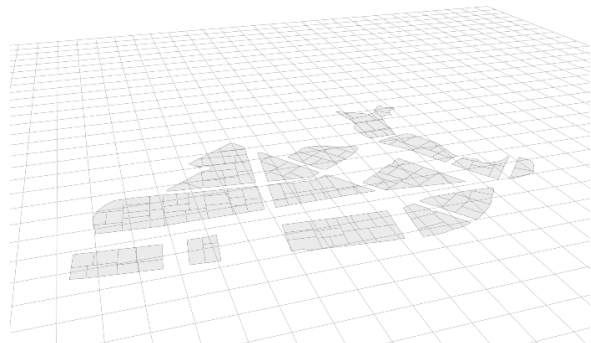
234 The steps of 3D modeling process in CityEngine are shown in Fig. 3. Based on the  
235 planning regulations and codes, recursive subdivision, which creates rectangular lots by  
236 repeatedly splitting the block, is applied to the zones with random seeds within the software,  
237 given the maximum and minimum lot area input. By this step, zones are subdivided into  
238 plots. In those plots, rectangular buildings are generated by using CGA rules with random  
239 height and site coverage values within certain intervals under the restrictions according to  
240 local practical regulations as shown in Table 1. Too small buildings with less than a  
241 footprint area of 300 m<sup>2</sup> are removed from the model. A 20% non-generation probability  
242 parameter is set for the simulation of open spaces.

243



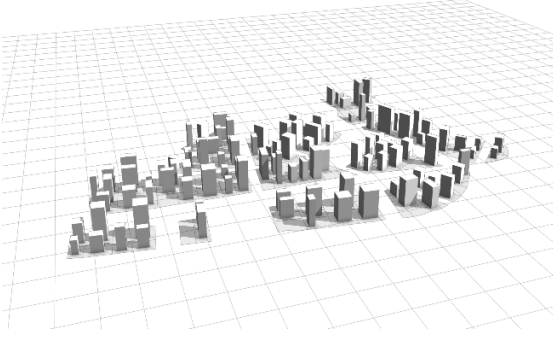
244

245 (a) Zoning data preparation



(b) Recursive plot subdivision

246



(c) CGA rule-based building extrusion

(d) Model alignment to terrain






**Fig. 3.** Rule-based parametric 3D modeling process in CityEngine

### 2.3 Geometric indicators calculation

To describe the neighborhood layout characteristics, several geometric indicators are calculated with reference to previous studies. The researchers have shown that several of them might have significant effects on different spatiotemporal occurrences such as sunlight access, urban heat island effect, heating and cooling loads [33-35]. Therefore, these important metrics described in Table 2 are used to characterize different aspects of neighborhood layout structure.

**Table 2.** Geometric indicators of neighborhood layout

Category	Metric	Description
General density and shape indicators	A_Height	Average building height (Unit: m) in every neighborhood layout case
	A_FootprintArea	Average building footprint area (Unit: m) in every neighborhood layout case
	A_Volume	Average building volume (Unit: m <sup>3</sup> ) in every neighborhood layout case
	A_AspectRatio	Average aspect ratio of building footprints in every neighborhood layout case
	A_StoV	Average building surface-to-volume ratio in every neighborhood layout case

Heterogeneity indicators	CV_Height	Coefficient of variation of building height in every neighborhood layout case	
	CV_FootprintArea	Coefficient of variation of building footprint area in every neighborhood layout case	
	CV_Volume	Coefficient of variation of building volume in every neighborhood layout case	
	CV_AspectRatio	Coefficient of variation of building footprint aspect ratio in every neighborhood layout case	
	CV_StoV	Coefficient of variation of building surface-to-volume ratio in every neighborhood layout case	

260

261       The characteristics of neighborhood layout are described by two aspects of metrics,  
262       one is the average value of density and shape parameters, and the other is the coefficient  
263       of variation value of density and shape parameters in each neighborhood case. The former  
264       indicators describe the general building characteristics in the neighborhood, and the latter  
265       ones represent the heterogeneity of neighborhood layout. Previous studies usually use the  
266       standard deviation of data to describe heterogeneity. In order to make a comparison of the  
267       impact of different heterogeneity indicators, this study adopts the coefficient of variation  
268       (CV), which is defined as the ratio of the standard deviation to the mean, instead of the  
269       standard deviation value. The CV is useful for comparing the degree of variation from one

indicator to another, even if the means are drastically different from one another.

## **2.4 Carbon emission simulation**

The carbon accounting scope adopted by this study is the embodied carbon emissions in the building operational stage. The emission sources include the direct emissions from the fuel combustion in stationary sources, and the energy indirect emissions of the purchased electricity and town gas. The carbon emission assessment process takes renewable energy collection into account. Both the carbon emission reduction potential from renewable energy collection and the net carbon emission considering building energy use-related emissions and emission reduction caused by renewable energy harvesting are examined and discussed in this study.

CitySim, a validated urban building energy modeling (UBEM) software, is applied to evaluate the renewable energy generation potential and thermal loads of the buildings in each generated neighborhood case. CitySim is one of the physics-based UBEM models which capture the full dynamic of building performance and offer the highest resolution, which provides with more accurate simulation results than the reduced-order models and data-driven models [3]. A radiation model based on the simplified radiosity algorithm (SRA), considering shading, long-wave radiant exchange between exterior surfaces, and short-wave solar reflection, is incorporated in CitySim. Compared with other physics-based models, CitySim reduces the simulation time as it employs a simplified simulation engine with optimization of urban form for cooling and heating demand assessment [36], which offers a good compromise between simplicity, accuracy and computational time [37]. The dual advantages match the need for efficiency and accuracy to evaluate hundreds of

neighborhood designs in the pre-planning process.

Only solar energy harvesting by the photovoltaic system is set for renewable energy generation in this research. Several scenarios have been set to simulate different levels of renewable energy adoption conditions, i.e., in rooftop, façade, and all surfaces configurations. This idea is taken into account since many prior studies have ignored alternative renewable energy sources (such as heat pumps, biomass, and wind turbines) in favor of exploring the trade-offs in passive solar urban architecture, which may be the most ideal for hot climatic conditions [7, 38].

The energy consumption of other end-use types apart from thermal loads and solar energy collection are estimated by the multiplication of local population and energy consumption per capita in the residential sector with reference to the Hong Kong Energy End-use Data. The carbon emissions of each energy end-use type are calculated by the emission factor in the local context for each kind of energy by multiplying the corresponding energy use volume. The total carbon emissions are the sum of the carbon emissions from each energy use type [39].

The simulation settings and carbon emission intensity are described in detail in the Appendices. The input parameter and settings for the building energy simulation in CitySim all refers to the general condition in the Hong Kong context.

## **2.5 Regression analysis**

In order to quantify the relationship between neighborhood layout heterogeneity and carbon emissions, ordinary least squares (OLS) multiple linear regression models are utilized. Two regression models are specified as follows:



$$316 \quad CE = \beta_0 + \beta_1 NoB + \beta_2 A\_Height + \beta_3 A\_FootprintArea + \beta_4 A\_Volume + \beta_5 A\_AspectRatio + \beta_6 A\_StoV + \varepsilon \quad (1)$$

$$317 \quad CE = \beta_0 + \beta_1 NoB + \beta_2 A\_Height + \beta_3 A\_FootprintArea + \beta_4 A\_Volume + \beta_5 A\_AspectRatio + \beta_6 A\_StoV + \beta_7 CV\_Height + \beta_8 CV\_FootprintArea + \beta_9 CV\_Volume + \beta_{10} CV\_AspectRatio + \beta_{11} CV\_StoV + \varepsilon \quad (2)$$

318 where CE is carbon emission reduction or net carbon emission volume,  $\beta_0$  is the intercepts  
 319 for all individuals,  $\beta_1$  to  $\beta_{11}$  are the intercepts for each individual, NoB stands for number  
 320 of buildings, the meaning of other variables such as A\_ Height has been described in detail  
 321 in Table 1, and  $\varepsilon$  denotes the random error. Equation (1) serves as a benchmark model  
 322 which only contains the general density and shape indicators and Equation (2) represents  
 323 an improved model which contains both density variables as controlled variables and  
 324 heterogeneity variables, in order to explore whether the heterogeneity variables can exert  
 325 influence on the interpretability of the regression model.

326 Before running the regression analysis, Pearson correlation analysis is used to pre-  
 327 explore the relationship among the neighborhood layout indicators, which aims at  
 328 preventing the strongly correlated independent variables from being put into the regression  
 329 model at the same time and resulting in the multicollinearity problem. The formula is  
 330 shown as follows:

$$331 \quad r = \frac{\sum_{i=1}^n (x_i - \bar{x})(y_i - \bar{y})}{\sqrt{\sum_{i=1}^n (x_i - \bar{x})^2} \sqrt{\sum_{i=1}^n (y_i - \bar{y})^2}} \quad (3)$$

332 where  $r$  is the Pearson correlation coefficient and represents the correlation degree,  $n$   
 333 stands for the sample size, and  $x_i$  and  $y_i$  are the individual sample points. The value of  $r$   
 334 is between  $-1$  and  $1$ .  $r = 1$  indicates a perfect positive relationship while  $r = -1$  implies  
 335 a perfect negative relationship between the variables.  $r = 0$  indicates that no linear

dependency exists between the two variables.

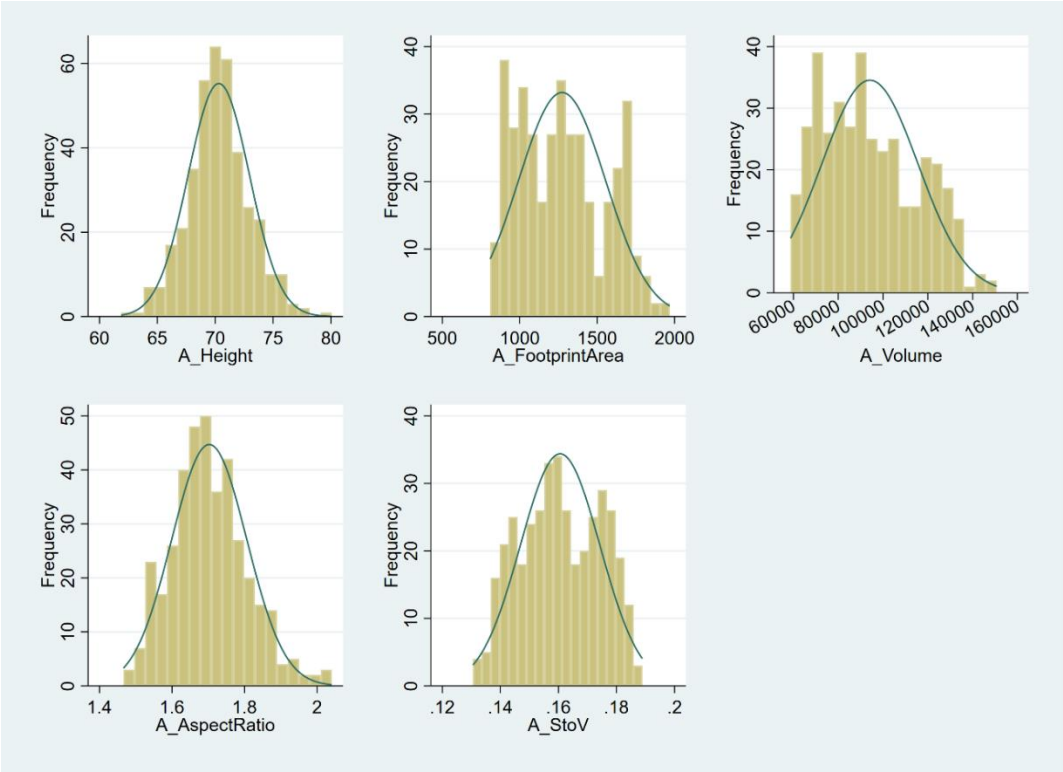
### **3 Results**

This study generates 384 neighborhood cases with different building layouts. The building geometry indicators are calculated through GIS software; The carbon emissions of the buildings of different photovoltaic installation scenarios in each layout case are simulated through CitySim. Then, the relationship between neighborhood layout heterogeneity and carbon emissions is explored through the OLS regression model. This section presents the results of the statistical characteristics of the variables explored in this study, and the relationship between neighborhood layout heterogeneity and carbon emissions obtained by the regression model.

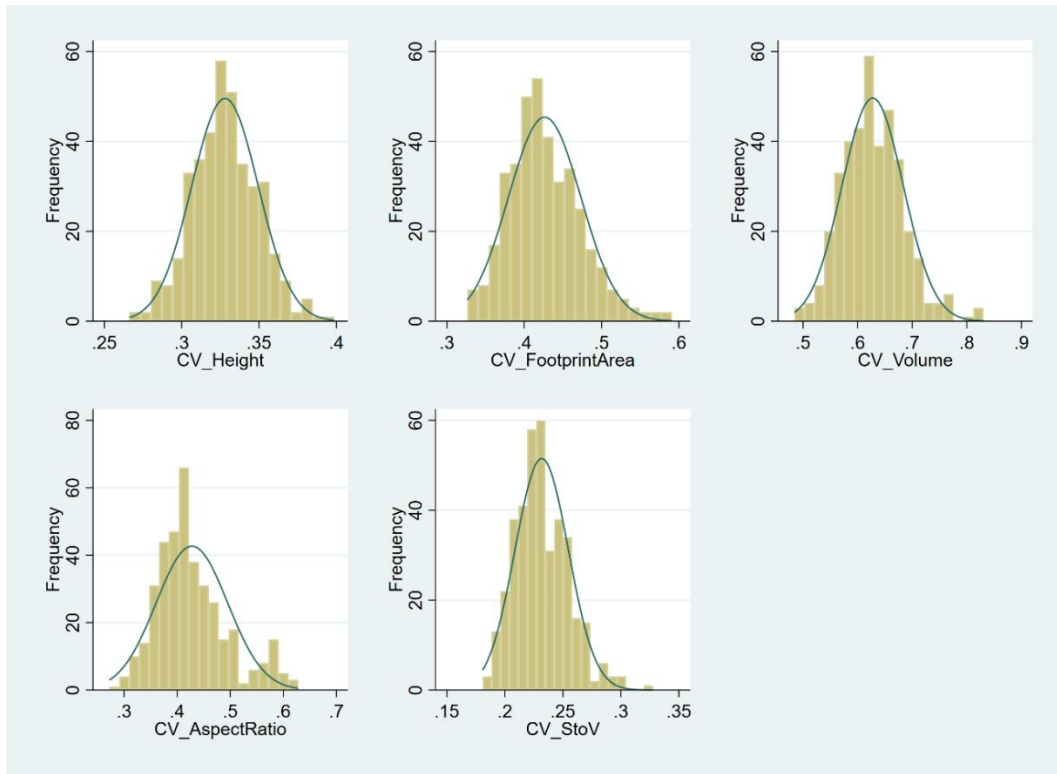
#### **3.1 Descriptive statistics of building geometry and carbon emissions**

Fig. 4 shows the distribution of the building geometry indicators of the generated 384 neighborhood layout cases, including the density and shape indicators in Fig. 4(a), and the heterogeneity indicators in Fig. 4(b). As most density and shape parameters presented in Fig. 4(a) are not directly controlled when generating the design variants, non-uniform distributions like the ones observed for most indicators are to be expected. However, the ranges spanned are good representations of what can be found in real, constructed neighborhoods [40]. The density and shape indicators, which are presented in Fig. 4(a) contain the average value of the height, footprint area, volume, aspect ratio, and the surface-to-volume ratio of the buildings in each generated layout case. Correspondingly, the heterogeneity indicators, as shown in Fig. 4(b), including the coefficient of variance value

of the height, footprint area, volume, aspect ratio, and the surface-to-volume ratio of the buildings in each generated layout case. Fig. 5 presents the distribution of carbon emission reduction (in Fig. 5(a)) and net carbon emissions regarding different photovoltaic installation scenarios (in Fig. 5(b)), which are generally both normally distributed.

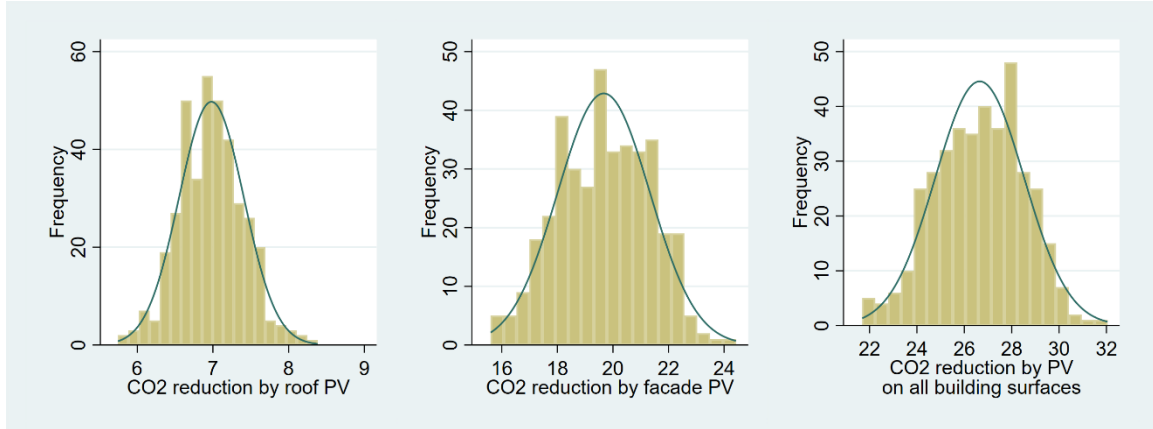


(a) Density and shape indicators of neighborhood layout

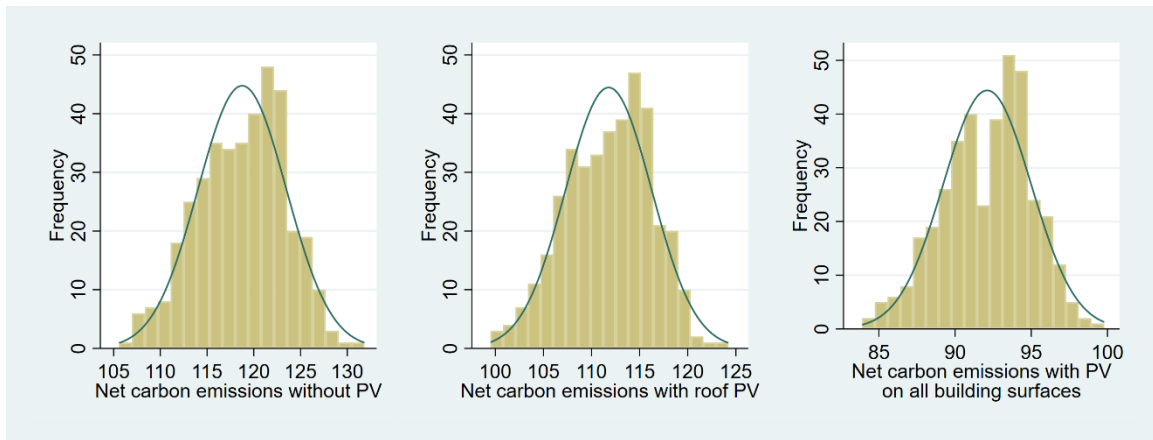


(b) Neighborhood layout heterogeneity indicators

**Fig. 4.** The distribution of neighborhood layout indicators



(a) Carbon emission reduction potential (Unit:  $10^6$  kg)



(b) Net carbon emissions (Unit:  $10^6$  kg)

**Fig. 5.** The distribution of carbon emissions under different PV installation scenarios

In order to further explore the distribution characteristics of the generated neighborhood layout and to avoid the collinearity in the regression model, the correlations among the neighborhood layout indicators are calculated and evaluated as Table 3 shows. In terms of the relationship between the density and shape indicators, it is notable that the average building volume shows a strong positive correlation with the average footprint area ( $r=0.986$ ). Besides, the average shape factor shows a strong negative correlation with the average footprint area ( $r=-0.979$ ) and building volume ( $r=-0.977$ ). These phenomena are caused by the plot division method applied in this study. In terms of the relationship among

the indicators of heterogeneity, most parameters show low or medium correlation with each other ( $|r| < 0.7$ ), except a strong positive correlation between the heterogeneity of building footprint area and building volume ( $r = 0.816$ ).

**Table 3.** Correlations among the neighborhood layout indicators

	A_ Height	A_ Footprint Area	A_ Volume	A_ Aspect Ratio	A_ StoV	CV_ Height	CV_ Footprint Area	CV_ Volume	CV_ Aspect Ratio	CV_ StoV
A_Height	1.000									
A_FootprintArea	0.086	1.000								
A_Volume	0.230	0.986	1.000							
A_AspectRatio	0.016	0.306	0.302	1.000						
A_StoV	-0.170	-0.979	-0.977	-0.266	1.000					
CV_Height	-0.558	0.033	-0.042	-0.010	0.059	1.000				
CV_FootprintArea	-0.057	-0.163	-0.152	-0.156	0.237	0.091	1.000			
CV_Volume	-0.374	-0.115	-0.135	-0.090	0.217	0.462	0.816	1.000		
CV_AspectRatio	0.069	0.493	0.492	0.626	-0.454	0.010	-0.025	-0.010	1.000	
CV_StoV	0.029	0.372	0.396	0.247	-0.287	0.129	0.456	0.406	0.320	1.000

Note: Positive correlations are marked in red, negative in blue. The light to dark color represents the weak to strong correlations.

Table 6 summarizes the descriptive statistics of the selected controlled variables, independent variables and dependent variables analyzed in the regression model. With the correlation test displayed in Table 3, the highly correlated variables are excluded from the regression models in order to avoid multicollinearity, such as A\_Volume (highly correlated with A\_FootprintArea), A\_StoV (highly correlated with A\_FootprintArea and A\_Volume), A\_AspectRatio (highly correlated with CV\_AspectRatio). After the exclusion, several density and shape indicators including the average value of the building height and footprint area, and the number of buildings are selected as controlled variables, all the heterogeneity indicators as the independent variables, and the carbon emissions of the

buildings in different photovoltaic installation scenarios in each layout case as dependent variables. The simulation results show that the solar energy generated by roof photovoltaic systems would account for around 6% carbon emission offset of the building in the neighborhood. The photovoltaic systems on the façade would lead to about 10% carbon emission offset. In terms of the heterogeneity indicators, the volume of the buildings in the generated neighborhood cases shows a relatively higher variation (average CV=0.638), while the building height and shape factor shows lower variations, with the average CV value of 0.328 and 0.232 respectively.

**Table 4.** Descriptive statistics of building geometry, and carbon emission reduction potential

	Unit	Min	Max	Mean	SD	N
<b>Dependent variables</b>						
Carbon reduction by roof PV	10 <sup>6</sup> kg	5.745	8.384	6.980	0.428	384
Carbon reduction by facade PV	10 <sup>6</sup> kg	15.600	24.426	19.670	1.660	384
Carbon reduction by PV on all building surfaces	10 <sup>6</sup> kg	21.693	32.043	26.650	1.873	384
Net carbon emissions without PV	10 <sup>6</sup> kg	105.592	131.830	118.755	4.727	384
Net carbon emissions with roof PV	10 <sup>6</sup> kg	99.499	124.212	111.775	4.482	384
Net carbon emissions with PV on all building surfaces	10 <sup>6</sup> kg	83.899	99.787	92.105	2.885	384
<b>Controlled variables</b>						
A_Height	m	61.887	80.061	70.313	2.653	384
A_FootprintArea	m <sup>2</sup>	809.230	1969.127	1273.609	281.752	384
Number of buildings	-	46.000	123.000	79.714	17.773	384
<b>Independent variables</b>						
CV_Height	-	0.266	0.399	0.328	0.022	384
CV_FootprintArea	-	0.327	0.591	0.426	0.047	384
CV_Volume	-	0.484	0.831	0.628	0.056	384
CV_AspectRatio	-	0.272	0.628	0.428	0.067	384
CV_StoV	-	0.181	0.328	0.232	0.023	384

### 3.2 The impact of neighborhood layout heterogeneity on carbon emission reduction resulting from solar energy harvesting by photovoltaic systems

Through the regression model, this section analyzes the association between the neighborhood layout heterogeneity and carbon emission reduction potential regarding different photovoltaic application scenarios. Three photovoltaic application scenarios are adopted: (1) the photovoltaic systems are applied on the building roofs; (2) the photovoltaic systems are applied on the building facades; (3) the photovoltaic systems are applied on all building surfaces including both roofs and facades. In the regression analysis of each scenario, we adopt one benchmark model which only contains the density variables and one improved model which contains both density variables as controlled variables and heterogeneity variables, in order to explore whether the heterogeneity variables can exert influence on the interpretability of the regression model.

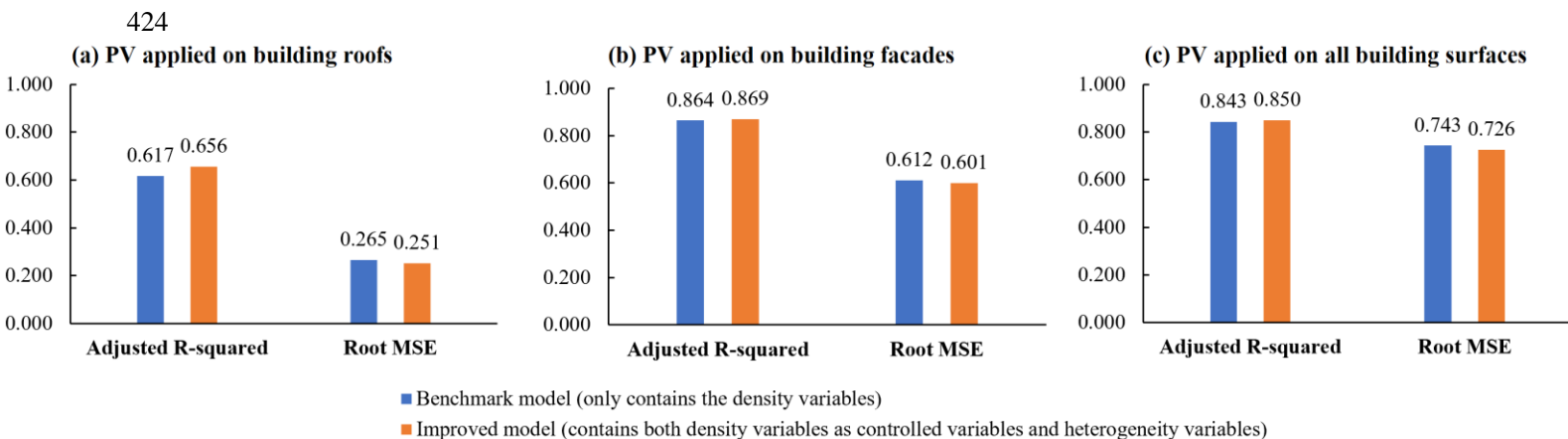


**Fig. 6** Performance metrics of the regression models that explores the impacts of heterogeneity indicators on carbon emission reduction potential with different PV application scenarios.

In terms of the performance of the regression models as displayed in Fig. 6, the



adjusted  $R^2$  of the improved models increases compared with that of the benchmark models, and the root MSE decreases, which means that adding the independent variables describing neighborhood layout heterogeneity to the regression models increases their goodness of fit and accuracy.

Table 5, Table 6, and Table 7 respectively present the regression results under the three scenarios. Under scenario 1, as shown in Table 5, two variables describing neighborhood layout heterogeneity including CV\_Height, and CV\_FootprintArea can exert a significant impact on the carbon reduction potential resulting from the solar harvesting by the photovoltaic system installation ( $p < 0.001$ ). CV\_Height has a significant negative impact on the carbon reduction potential in the whole neighborhood ( $B = -3.126$ ,  $p < 0.001$ ), as the heterogeneity of building height leads to lower solar radiation on building roofs caused by more mutual shading among the buildings. Additional  $5.684 \times 10^5$  kwh energy can be produced from the roof PV system by the decrease of 0.1 CV\_Height in the case study area, thus leading to  $3.126 \times 10^5$  kg carbon reduction. On the contrary, CV\_FootprintArea has a significant positive impact on the carbon reduction potential in the whole neighborhood ( $B = 1.317$ ,  $p < 0.001$ ), which indicating that given certain height heterogeneity, the heterogeneous building footprint area would reduce the mutual shading among buildings in the high-density area. The 0.1 rise of CV\_FootprintArea can bring  $1.395 \times 10^5$  kwh additional energy production from roof PV energy collection and thus  $1.317 \times 10^5$  kg carbon reduction potential. Comparing the standardized coefficients (Beta) of CV\_Height (Beta = -0.157) and CV\_FootprintArea (Beta = -0.145), it is found that they have similar strength of effects on the carbon emission reduction potential.

**Table 5.** Regression results of the association between neighborhood layout heterogeneity and carbon emission reduction potential when the photovoltaic systems are applied on the building roofs

<i>Dependent variable: Carbon reduction by roof PV</i>							
	<i>Unstandardized coefficients</i>		<i>Standardized coefficients</i>			<i>95% confidence interval for B</i>	
	<b>B</b>	<b>Std. err.</b>	<b>Beta</b>	<b>t</b>	<b>Sig.</b>	<b>Lower bound</b>	<b>Upper bound</b>
<b>Benchmark Model</b>							
A_FootprintArea	0.004	0.000	2.312	24.760	0.000	0.003	0.004
Number of buildings	0.054	0.002	2.245	24.040	0.000	0.050	0.058
(Constant)	-1.797	0.355		-5.070	0.000	-2.495	-1.100
<b>Improved Model</b>							
<i>Controlled variables</i>							
A_FootprintArea	0.004	0.000	2.337	25.600	0.000	0.003	0.004
Number of buildings	0.054	0.002	2.242	24.690	0.000	0.050	0.058
<i>Independent variables</i>							
CV_Height	-3.126	0.606	-0.157	-5.160	0.000	-4.317	-1.935
CV_FootprintArea	1.317	0.282	0.145	4.670	0.000	0.763	1.870
(Constant)	-1.377	0.452		-3.050	0.002	-2.265	-0.488

Under scenario 2, which explores the effects of neighborhood layout heterogeneity on carbon reduction potential caused by solar energy harvesting of building façades as shown in Table 6, CV\_AspectRatio and CV\_StoV are found to be significantly related to the dependent variable ( $p < 0.05$ ). Both of them positively affect carbon emission reduction. When CV\_AspectRatio in the neighborhood increases 0.1, the energy production from facade PV solar energy harvesting rises  $2.795 \times 10^5$  kwh, and the carbon reduction potential increases  $1.537 \times 10^5$  kg in the case-study neighborhood; CV\_StoV rising 0.1, energy production would increase  $6.113 \times 10^5$  kwh, and carbon reduction potential increases  $3.362 \times 10^5$  kg. This result indicates that the variation of building shape in a neighborhood in high-density areas would decrease the mutual shading and increase the solar harvesting

potential of building facades.

**Table 6.** Regression results of the association between neighborhood layout heterogeneity and carbon emission reduction potential when photovoltaic systems are applied on the building facades

<i>Dependent variable: Carbon reduction by facade PV</i>							
	<i>Unstandardized coefficients</i>		<i>Standardized coefficients</i>			<i>95% confidence interval for B</i>	
	<b>B</b>	<b>Std. err.</b>	<b>Beta</b>	<b>t</b>	<b>Sig.</b>	<b>Lower bound</b>	<b>Upper bound</b>
<b>Benchmark Model</b>							
A_Height	0.198	0.012	0.316	16.790	0.000	0.175	0.221
Number of buildings	0.082	0.002	0.876	46.530	0.000	0.078	0.085
(Constant)	-0.762	0.842		-0.910	0.366	-2.417	0.893
<b>Improved Model</b>							
<i>Controlled variables</i>							
A_Height	0.194	0.012	0.311	16.760	0.000	0.172	0.217
Number of buildings	0.086	0.002	0.924	42.040	0.000	0.082	0.090
<i>Independent variables</i>							
CV_AspectRatio	1.537	0.530	0.062	2.900	0.004	0.495	2.579
CV_StoV	3.362	1.464	0.047	2.300	0.022	0.482	6.242
(Constant)	-2.318	0.922		-2.510	0.012	-4.131	-0.505

Under scenario 3, when the photovoltaic systems have been applied to all the building surfaces, the regression results are described in Table 7. The heterogeneity of building density and shape, including CV\_Height, CV\_Volume, and CV\_StoV, can significantly affect the carbon emission reduction potential caused by the solar energy harvesting of all the building surfaces. Similar to the effect under scenario 1, the heterogeneity of building height results in a significant negative impact on carbon reduction potential (B=-5.526, p=0.009). The 0.1 decrease of CV\_Height would result in

the increase of  $1.005 \times 10^6$  kwh energy production and  $5.526 \times 10^5$  kg carbon reduction by PV energy collection on all building surfaces in the case-study area. In contrast, the heterogeneity of building surface-to-volume ratio ( $B=5.399$ ,  $p=0.012$ ) improve the carbon reduction potential. With CV\_StoV rising 0.1, energy production from solar harvesting on all building surfaces gains  $9.816 \times 10^5$  kwh and carbon reduction  $5.399 \times 10^5$  kg. In terms of the strength of the effect of these three independent variables, CV\_Height ( $Beta=-0.064$ ) would have a similar strength of impact compared with CV\_StoV ( $Beta=0.066$ ).

**Table 7.** Regression results of the association between neighborhood layout heterogeneity and carbon emission reduction potential when photovoltaic systems have been applied on the building surfaces including both roofs and facades

<i>Dependent variable: Carbon reduction by PV on all building surfaces</i>							
	<i>Unstandardized coefficients</i>		<i>Standardized coefficients</i>			<i>95% confidence interval for B</i>	
	<b>B</b>	<b>Std. err.</b>	<b>Beta</b>	<b>t</b>	<b>Sig.</b>	<b>Lower bound</b>	<b>Upper bound</b>
<b>Benchmark Model</b>							
A_Height	0.181	0.015	0.026	12.260	0.000	0.152	0.209
A_FootprintArea	0.007	0.000	0.988	16.060	0.000	0.006	0.007
Number of buildings	0.181	0.006	1.723	28.090	0.000	0.169	0.194
(Constant)	-8.875	1.275		-6.960	0.000	-11.383	-6.368
<b>Improved Model</b>							
<i>Controlled variables</i>							
A_Height	0.154	0.017	0.218	8.890	0.000	0.120	0.188
A_FootprintArea	0.007	0.000	0.983	15.670	0.000	0.006	0.007
Number of buildings	0.185	0.006	1.752	28.760	0.000	0.172	0.197
<i>Independent variables</i>							
CV_Height	-5.526	2.110	-0.064	-2.620	0.009	-9.675	-1.377
CV_FootprintArea	0.833	0.979	0.021	0.850	0.396	-1.093	2.759
a							
CV_AspectRatio	0.959	0.645	0.034	1.490	0.138	-0.308	2.227
CV_StoV	5.399	2.148	0.066	2.510	0.012	1.176	9.622
(Constant)	-7.395	1.914		-3.860	0.000	-11.158	-3.631

In general, vertical heterogeneity of building layout (i.e. higher coefficient of variance of building height) would impede the carbon emission reduction potential of a high-density neighborhood, while horizontal heterogeneity of building layout (i.e. higher coefficient of variance of building footprint area) could improve the carbon emission reduction potential. It is notable that the heterogeneity of building shape factor (i.e. higher coefficient of variance of building aspect ratio and surface-to-volume ratio) is helpful in carbon reduction, especially for the solar energy collection of building façades.

### **3.3 The impact of neighborhood layout heterogeneity on net carbon emission**

The net carbon emissions considering the balance of building energy use and energy generation through the photovoltaic systems regarding different installation scenarios are set as the dependent variables in this section. The scenarios set in this section are different from those in 3.2, as the condition that the photovoltaic system being installed only on building facades but not on roofs is basically impossible to be adopted in reality. So, the scenarios set in this section include: (1) no photovoltaic systems are applied on the buildings; (2) the photovoltaic systems are applied on the building roofs; (3) the photovoltaic systems are applied on all building surfaces including both roofs and facades. Table 7, Table 8, and Table 9 respectively present the relationship between the net carbon emissions and the neighborhood layout heterogeneity under these three scenarios.

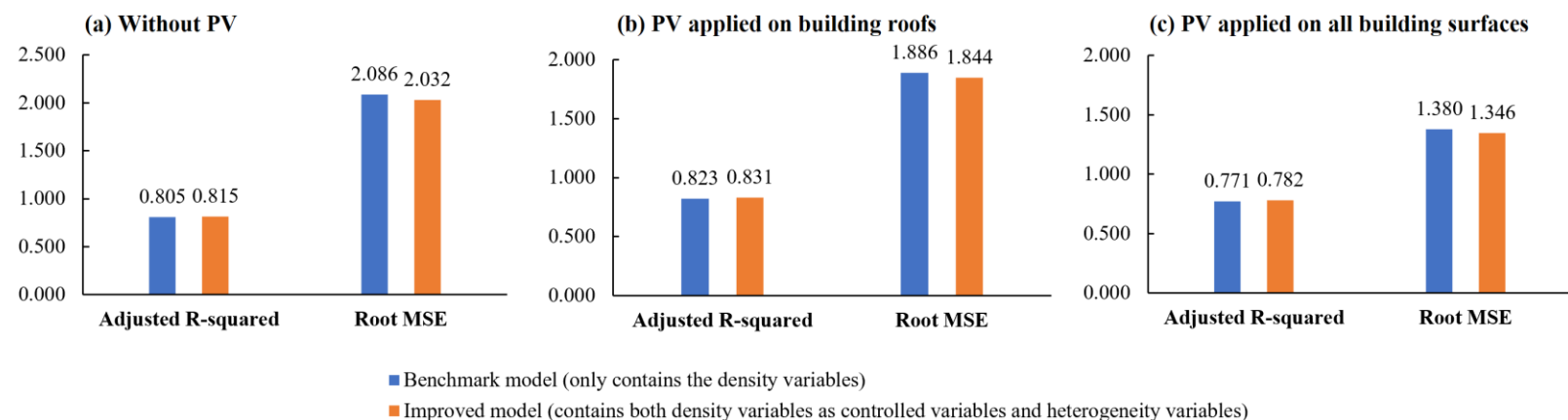


**Fig. 7** Performance metrics of the regression models that explores the impacts of heterogeneity indicators on net carbon emissions with different PV application scenarios

In terms of the general performance of the regression models, as shown in Fig. 7 compared with the benchmark models, the adjusted  $R^2$  increases, and the root MSE reduces in the improved model under all the scenarios, which means that adding the independent variables describing neighborhood layout heterogeneity to the regression models increases their goodness of fit and accuracy.

Looking into the variables, as the carbon emission offset resulting from the solar energy collection only accounts for less than 10% of the total carbon emissions of the buildings in a neighborhood, the effect of the independent variables describing neighborhood layout heterogeneity has a similar effect on the net carbon emissions among the three scenarios. For all three scenarios, the heterogeneity of building height can lead to significantly lower carbon emissions (at least at  $p < 0.01$  level), while the heterogeneity of building volume (at least at  $p < 0.05$  level) and surface-to-volume ratio (at least at  $p < 0.05$  level) would cause significantly higher carbon emissions.

Under scenario 1, the dependent variable is the net carbon emissions of buildings without carbon offset from solar harvesting, thus the emissions are all from building energy

consumption. The heterogeneity of building height plays an important role to reduce energy consumption ( $B=-17.824$ ,  $p=0.004$ ), the reason for which might be the higher mutual shading under this circumstance give rise to less cooling loads of the buildings [25]. Without PV installation, when CV\_Height raises 0.1, the net carbon emissions in the case-study area correspondingly increases  $1.782 \times 10^6$  kg. The heterogeneity of the shape of the buildings in a neighborhood would cause higher carbon emissions due to less mutual shading ( $B=14.131$ ,  $p=0.014$ ). When CV\_Height raises 0.1, the net carbon emissions in the case-study area gains  $1.413 \times 10^6$  kg. Under scenario 2 and scenario 3, the impacts of the independent variable are similar to that under scenario 1 because of the small share of carbon emission offset from the photovoltaic systems, though the strength of impact slightly changes. In detail, with the roof PV system,  $1.737 \times 10^6$  kg carbon emissions can be avoided with 0.1 rise of CV\_Height, while additional  $1.434 \times 10^6$  kg carbon emissions are generated from the 0.1 increase of CV\_StoV. Under the circumstance that the PV systems have been applied to all building surfaces,  $1.345 \times 10^6$  kg carbon emissions can be avoided through the increase of 0.1 CV\_Height, and  $9.634 \times 10^5$  carbon emissions would be brought by the 0.1 increase of CV\_StoV.

**Table 8.** Regression results of the association between neighborhood layout heterogeneity and net carbon emissions without photovoltaic system installation

<i>Dependent variable: Net carbon emissions without PV</i>							
	<i>Unstandardized coefficients</i>		<i>Standardized coefficients</i>			<i>95% confidence interval for B</i>	
	<b>B</b>	<b>Std. err.</b>	<b>Beta</b>	<b>t</b>	<b>Sig.</b>	<b>Lower bound</b>	<b>Upper bound</b>
<b>Benchmark Model</b>							
A_Height	0.560	0.041	0.314	13.530	0.000	0.478	0.641
A_FootprintArea	0.017	0.001	0.993	14.510	0.000	0.014	0.019
Number of buildings	0.445	0.018	1.675	24.550	0.000	0.410	0.481
(Constant)	22.682	3.581		6.330	0.000	15.640	29.724
<b>Improved Model</b>							
<i>Controlled variables</i>							
A_Height	0.513	0.049	0.288	10.390	0.000	0.416	0.610
A_FootprintArea	0.017	0.001	1.003	14.840	0.000	0.015	0.019
Number of buildings	0.452	0.018	1.699	25.410	0.000	0.417	0.487
<i>Independent variables</i>							
CV_Height	-17.824	6.216	-0.081	-2.870	0.004	-30.047	-5.602
CV_Volume	4.929	2.466	0.059	2.000	0.046	0.080	9.779
CV_StoV	14.131	5.722	0.069	2.470	0.014	2.879	25.382
(Constant)	24.696	5.373		4.600	0.000	14.131	35.261



**Table 9.** Regression results of the association between neighborhood layout heterogeneity and net carbon emissions when photovoltaic systems have been applied on the building roofs

<i>Dependent variable: Net carbon emissions with roof PV</i>							
	<i>Unstandardized coefficients</i>		<i>Standardized coefficients</i>			<i>95% confidence interval for B</i>	
	<b>B</b>	<b>Std. err.</b>	<b>Beta</b>	<b>t</b>	<b>Sig.</b>	<b>Lower bound</b>	<b>Upper bound</b>
<b>Benchmark Model</b>							
A_Height	0.550	0.037	0.326	14.720	0.000	0.477	0.624
A_FootprintArea	0.013	0.001	0.831	12.730	0.000	0.011	0.015
Number of buildings	0.392	0.016	1.555	23.910	0.000	0.360	0.425
(Constant)	24.978	3.238		7.710	0.000	18.612	31.344
<b>Improved Model</b>							
<i>Controlled variables</i>							
A_Height	0.537	0.047	0.318	11.520	0.000	0.445	0.629
A_FootprintArea	0.013	0.001	0.812	12.120	0.000	0.011	0.015
Number of buildings	0.393	0.016	1.560	23.910	0.000	0.361	0.426
<i>Independent variables</i>							
CV_Height	-17.372	6.279	-0.083	-2.770	0.006	-29.718	-5.025
CV_Volume	9.253	4.178	0.116	2.210	0.027	1.039	17.468
CV_StoV	14.335	5.391	0.074	2.660	0.008	3.734	24.935
CV_FootprintArea	-6.906	4.642	-0.072	-1.490	0.138	-16.034	2.221
a							
(Constant)	25.706	4.876		5.270	0.000	16.118	35.294

**Table 10.** Regression results of the association between neighborhood layout heterogeneity and net carbon emissions when photovoltaic systems have been applied on the building surfaces including both roofs and facades

<i>Dependent variable: Net carbon emissions with PV on all building surfaces</i>							
	<i>Unstandardized coefficients</i>		<i>Standardized coefficients</i>			<i>95% confidence interval for B</i>	
	<b>B</b>	<b>Std. err.</b>	<b>Beta</b>	<b>t</b>	<b>Sig.</b>	<b>Lower bound</b>	<b>Upper bound</b>
<b>Benchmark Model</b>							
A_Height	0.379	0.027	0.349	13.850	0.000	0.325	0.433
A_FootprintArea	0.010	0.001	0.986	13.280	0.000	0.009	0.012
Number of buildings	0.264	0.012	1.626	21.980	0.000	0.240	0.288
(Constant)	31.557	2.370		13.310	0.000	26.897	36.218
<b>Improved Model</b>							
<i>Controlled variables</i>							
A_Height	0.363	0.034	0.334	10.680	0.000	0.296	0.430
A_FootprintArea	0.010	0.001	0.960	12.620	0.000	0.008	0.011
Number of buildings	0.267	0.012	1.643	22.200	0.000	0.243	0.290
<i>Independent variables</i>							
CV_Height	-13.453	4.574	-0.100	-2.940	0.003	-22.446	-4.460
CV_Volume	6.575	3.043	0.128	2.160	0.031	0.591	12.559
CV_StoV	9.634	3.976	0.077	2.420	0.016	1.817	17.452
CV_AspectRatio	-4.237	3.384	-0.069	-1.250	0.211	-10.892	2.417
(Constant)	1.828	1.193		1.530	0.126	-0.519	4.175

## 4 Discussion

This study explores the impact of neighborhood layout heterogeneity on building carbon emissions. The results provide references for neighborhood layout design in high-density cities, especially supporting the pre-design process.

### 4.1 A GIS-based parametric method for neighborhood layout cases generation and carbon emission assessment

This study applies a parametric method in a real planning zone to generate neighborhood layout cases for further carbon emission assessment. This method retains the basic development setting in the real world (e.g., zoning plan, development restriction, and

building planning regulations), which leads to quasi-experiments instead of true experiments rigorously controlled by researchers as those performed in laboratories [41]. Besides, it enables the comparison of household energy in settings with various densities and configurations. It provides an efficient tool to generate a large number of cases at one time for the discovery of the “best” case. However, it should be noted that the planning and design process of neighborhood layout in real-world practice would be much more complicated than what is designed in this research. Building placement affected by topography, shading and ventilation standard should all be taken into consideration and strictly controlled in the neighborhood layout design. Despite this, the parametric method is still a powerful tool that can support building layout design, especially in the pre-design process.

Several parametric tools have been applied to generate parametric building clusters for environmental-targeted planning in previous studies, including grasshopper in Rhino, CitySketch in Blender and CityEngine. CityEngine is a GIS-based software produced by Esri. It can be well connected to ArcGIS, which is a widely accepted software for urban planning not only in the research field but also in real practice. The application of CityEngine on neighborhood design can fit well into other GIS urban-scale data processing and support the whole urban planning process.

#### **4.2 The relationship between neighborhood layout heterogeneity and carbon emission**

The results of this study show that the neighborhood layout heterogeneity in high-density areas can exert significant influences on carbon emissions from buildings. The carbon emissions come from the building energy consumption deducting the emission offset from renewable energy infrastructure and carbon sinks (e.g. greening, waterbody,

and so on). In the high-density area, the interaction between buildings would change the micro-climate and thus affect energy use and carbon emissions.

This study explores both the impact of urban heterogeneity on the carbon emission reduction potential resulting from solar harvesting by photovoltaic panels and the net carbon emissions considering both energy use and energy offset. This study acknowledges that the arbitrary placement of horizontal and vertical structures in urban form can significantly impair the potential for urban solar energy.

In terms of the carbon reduction potential, the results show that the heterogeneity of building height can lead to lower carbon reduction potential because of more mutual shading on the building roofs. On the contrary, the heterogeneity of shape factor (i.e. building aspect ratio and surface-to-volume ratio) can improve the carbon reduction potential because the heterogeneous distribution of the buildings avoids mutual shading between the buildings and lead to the more solar exposure area.

By taking both building energy use and energy offset by photovoltaic panels, the net carbon emissions are examined. When exploring the influence factors on net carbon emissions, the effects of neighborhood layout heterogeneity are similar to that on the carbon reduction potential, that is to say, the un-uniform building height reduces building energy consumption while the un-uniform building shape increases building energy use. A possible explanation for these results might be also related to the shading effect. As Hong Kong is located in the sub-tropical area, and a large share of building energy use results from the cooling loads. Higher mutual shading contributes to less cooling loads and thus lower energy consumption. These results support the previous research, in which the high-low mixed-rise building cluster holds higher solar potential than the pure high-rise building

cluster in high-density areas [24].

It is worth noticing that the neighborhood layout heterogeneity settings to maximize building solar energy harvesting and minimize building energy consumption are contradictory to each other. The regression results show that the setting of photovoltaic panels could lead to limited effects on the relationship between urban heterogeneity and net carbon emissions, because the carbon reduction resulting from solar harvesting only accounts for a small share compared to the total carbon emissions in the neighborhood. Under this circumstance, the interrelationship between the carbon reduction from solar energy harvesting and net carbon emissions is eclipsed by building energy use. Actually, the assumptions of the photovoltaic parameters (e.g., material type, dimension, and solar cell efficiency) adopted in this study are based on the existing technology levels and commercial availability. However, with the development of photovoltaic technology and the improved solar harvesting capability, the carbon emission offset by those kinds of renewable energy infrastructures would raise and occupy a higher share of the total net carbon emissions in the future. How to balance solar harvesting and building energy consumption would be a new question, which need not only more exploration on the definition and classification of neighborhood heterogeneity, but also the efficient simulation software integrating the more accurate neighborhood micro-climate context, especially with the coupling of Computational Fluid Dynamics and thermoradiative model to assess the effect of the changing wind flow caused by various building distribution and building energy consumption.

#### **4.3 Implications for neighborhood layout planning in high-density cities**

637           The methodology and results of this study can provide implications in low-carbon  
638 neighborhood layout planning and design in high-density cities, especially for a new  
639 development area.

640           In the pre-design process of a new development neighborhood, it is necessary to  
641 propose various schemes and assess their environmental performances. This study provides  
642 with an efficient method based on the GIS tool to quickly generate multiple kinds of  
643 planning schemes while following the development restrictions proposed in the planning  
644 documents. This process offers the opportunity to integrate the building model design and  
645 generation with other GIS urban-scale data processing, which brings convenience for urban  
646 planning compared with the building generation in other stand-alone software (e.g., CAD,  
647 Blender, and Rhinoceros).

648           Another implication comes from the regression results on how to design specific  
649 neighborhood layout patterns with lower carbon emissions. The results emphasize the  
650 importance of the building height uniformity instead of heterogeneity to maximize roof  
651 solar energy harvesting, and the building shape heterogeneity to maximize façade solar  
652 exposure. It is also found that these two characteristics would reduce building energy  
653 consumption. Therefore, when designing the building layout, it is a key issue for the  
654 practitioners to balance the two sides. How to design proper building density, shape, and  
655 arrangement in a neighborhood to increase solar energy collection and reduce building  
656 energy consumption while also creating a comfortable living environment, should be paid  
657 attention to in future studies. Besides, with the development of green building technology,  
658 the interaction between neighborhood layout and carbon emissions would also change  
659 accordingly.

#### 4.4 Limitations and future research

Several limitations of this research should be addressed in future investigations. Firstly, the findings of this study are based on the simplified building structure. The buildings generated for carbon emission simulation are all set as simple cuboids with flat roofs and flat-installed PV panels. Complex building shapes, attached structures, and shading devices have not been taken into consideration. Besides, the several scenarios of different PV installations all assume the same ratio and evenly distributed PV panels of all the buildings. These simplifications of building models greatly reduce simulation time but might cause inaccuracy in the simulation results compared with that in the real world. Another problem caused by these simple assumptions is that the results overestimate the carbon reduction by solar energy harvesting, as the building surfaces failing to meet the solar radiation threshold would not adopt PV panels in real practice for cost efficiency consideration. In future studies, more refined building geometry and a pre-analysis to identify the building surface that meet the PV installation standard regarding solar radiation threshold shall be adopted to raise the accuracy of the carbon emission assessment. Additionally, the energy use efficiency improvement of buildings with the technical upgrading are suggested to be taken into account in the future [42]. Meanwhile, the cost efficiency of various green building technology should be considered.

Secondly, this research only probes into the neighborhood-scale total carbon emissions and the general neighborhood layout heterogeneity. The research scope could be refined to a more detailed one in order to get a comprehensive understanding of the interaction between neighborhood layout heterogeneity and carbon emissions. The solar

683 harvesting on building facades of different orientations, and the heterogeneity under  
684 different building arrangement patterns and height distribution patterns (e.g. stepped  
685 building height) should be further examined. Besides, in planning and design practices, the  
686 layout indicators may affect each other and also have an interaction effect on carbon  
687 emissions. Therefore, further work is required to integrate the interaction terms of the  
688 indicators into the regression model to examine the interaction effect of two or even more  
689 heterogeneity indicators on carbon emissions. Path analysis is also needed to investigate  
690 the directed dependencies among a set of neighborhood layout indicators.

691         Thirdly, the research scope of this study only covers the emissions from buildings,  
692 without the investigation of the carbon emissions from traffic, waste treatment, and carbon  
693 sequestration from vegetations. The placement of the buildings might affect the traffic  
694 emissions. Besides, the vegetation system might one on hand mitigate the urban heat island  
695 effect and reduce the emissions from the buildings' cooling loads [43], on the other hand  
696 serve as the carbon sink absorbing carbon from the atmosphere. Future studies are  
697 suggested to take these emission sources into consideration, thus capturing a whole picture  
698 about the relationship between urban form and total carbon emissions.

699         Moreover, whether the results and implications can be generalized to other  
700 neighborhoods, other climatic contexts, and future scenarios should be further investigated.  
701 This study chooses one new development area in Hong Kong as the case study area. The  
702 planning plots are pre-defined by the planning scheme. The selected site with the pre-  
703 defined plots has its specialty, which might restrict the generalization to other areas. Future  
704 studies are supposed to expand the exploration to other areas and make comparison studies  
705 so as to further ascertain the applicability of the findings.



## 5 Conclusion

A paradigm shift toward low-carbon urban design has broad support in the context of climate change. In order to have a better understanding of sustainable neighborhood design, prior research has investigated the effect of neighborhood layout design on environmental performance especially carbon emissions; however, they concentrated on density characteristics while ignoring the neighborhood's rational building arrangement, particularly the layout heterogeneity, which would lead to various environmental performance outcomes under the complex and dynamic interaction among buildings. In spite of a few studies addressed the above research topic, the exploration of spatial heterogeneity indicators focuses on building height diversity, while ignoring the building shape variation. They fail to systematically demonstrate the relationship between neighborhood layout heterogeneity and carbon emissions. Additionally, past research looked at the various planning and geometry aspects separately rather than considering how they could interact. To fill the research gap, the current paper systematically explores the impact of five neighborhood layout heterogeneity indicators includes the coefficient of variation of building height, footprint area, volume, aspect ratio, and surface-to-volume ratio on carbon emissions, with consideration of several scenarios regarding different renewable energy application ratios. The joint effects of the geometric indicators are analyzed by multiple regression models.

A prototype high-density neighborhood is designed in Hong Kong, based on the synthesis of recommendations in available guidelines for sustainable communities, and on existing standards of development restriction proposed in the planning documents for the

selected region. The design takes the different scenarios of renewable energy infrastructure adoption into consideration, providing insights into the balance of minimizing building energy consumption and maximizing the renewable energy collection in neighborhood planning. The neighborhood heterogeneity is described by the coefficient of variation of building density and shape factors. The coefficient of variation makes it comparable among the different neighborhood layout heterogeneity indicators.

The results of this study highlight that the heterogeneity of building density and shape can lead to a significant impact on neighborhood carbon emissions. The heterogeneity of building height results in less mutual shading on building roofs and thus more carbon reduction for the neighborhood from solar energy harvesting. On the contrary, the carbon reduction by building façade solar energy collection could be improved by the heterogeneity of building shape, including a variation of aspect ratio and surface-to-volume ratio. When considering both energy consumption and renewable energy collection, the heterogeneity of building height and uniformity of building shape can lead to less net carbon emissions. It is notable that in high-density areas, the uniformity of neighborhood layout design would lead to the opposite result in carbon reduction efforts regarding solar energy collection and building energy consumption. Under the condition of the existing PV technology, the heterogeneity of building height and uniformity of building shape factors would be more favorable for low-carbon neighborhood planning.

In conclusion, this study provides a systematic understanding of the relationship between neighborhood layout heterogeneity and environmental performance. It also provides urban planners an efficient GIS-based tool to generate multiple kinds of neighborhood layouts and perform an initial estimation of the carbon emissions. Whilst

Hong Kong is chosen as a case study city, the methodology and results in this study can be extrapolated to other tropical high-density regions.

## Appendices

**Table A1.** Simulation parameter settings in CitySim [30, 44-46]

Category		Settings
Climate		Hong Kong
Infiltration and temperature	Infiltration	0.26 h <sup>-1</sup>
	T max	26 °C
	Shading device	0.2
	Cut-off irradiance	100
Opening properties	Glazing ratio	0.4
	U-value	0.67
	g-value	0.65
	Openable fraction	0.99
Occupants	Number	118000
	Sensible heat	90 W/p
	Radiant part	0.6
	Latent heat	60 W/p
PV panel	Name	1Soltech 1STH-235-WH
	Type	Mono-c-Si

**Table A2.** The construction materials of building envelope settings in CitySim [47, 48]

Layer	Thickness (m)	Material	Thermal conductivity (W/mK)	Density (kg/m3)	Specific heat (J/kgK)
<b>Wall</b>					
Layer 1	0.005	Mosaic Tiles	1.5	2500	840
Layer 2	0.01	Cement/Sand Plastering	0.72	1860	840
Layer 3	0.1	Heavy Concrete	2.16	2400	840
Layer 4	0.01	Gypsum Plastering	0.38	1120	840
<b>Roof</b>					
Layer 1	0.025	Concrete Tiles	1.1	2100	920
Layer 2	0.02	Asphalt	1.15	2350	1200
Layer 3	0.05	Cement/Sand Screed	0.72	1860	840
Layer 4	0.05	Expanded Polystyrene	0.034	25	1380
Layer 5	0.15	Heavy Concrete	2.16	2400	840
Layer 6	0.01	Gypsum Plaster	0.38	1120	840
<b>Floor</b>					
Layer 1	0.01	Gypsum Plasterboard	0.38	1120	837
Layer 2	0.18	Reinforced Concrete	1.9	2300	840
Layer 3	0.01	Floor Tiles	0.8	1700	850
<b>Ground</b>					
Layer 1	1.00	Vegetation	0.52	2000	1840

**Table A3.** Carbon emission factors and intensity of energy in Hong Kong [49-51]

Energy	Direct emission factor	Indirect emission intensity	Unit
LPG	3.017		kg/kg
Towngas	2.549	0.588	kg/unit
Electricity (from CLP)		0.390	kg/kWh
Electricity (from HEC)		0.710	kg/kWh

## References

- [1] International Energy Agency. Empowering Cities for a Net Zero Future: Unlocking resilient, smart, sustainable urban energy systems. France2021.
- [2] Butera FM. 1.3 - Sustainable Neighborhood Design in Tropical Climates. In: Droege P, editor. Urban Energy Transition (Second Edition): Elsevier; 2018. p. 51-73.
- [3] Hong TZ, Chen YX, Luo X, Luo N, Lee SH. Ten questions on urban building energy modeling. Building and Environment. 2020;168.
- [4] Alavipanah S, Schreyer J, Haase D, Lakes T, Qureshi S. The effect of multi-dimensional indicators on urban thermal conditions. Journal of Cleaner Production. 2018;177:115-23.
- [5] Han YL, Taylor JE, Pisello AL. Exploring mutual shading and mutual reflection inter-building effects on building energy performance. Applied Energy. 2017;185:1556-64.
- [6] Huo TF, Ma YL, Xu LB, Feng W, Cai WG. Carbon emissions in China's urban residential building sector through 2060: A dynamic scenario simulation. Energy. 2022;254.
- [7] Zhang J, Xu L, Shabunko V, Tay SER, Sun HX, Lau SSY, et al. Impact of urban block typology on building solar potential and energy use efficiency in tropical high-density city. Applied Energy. 2019;240:513-33.
- [8] Hachem C, Athienitis A, Fazio P. Evaluation of energy supply and demand in solar neighborhood. Energ Buildings. 2012;49:335-47.
- [9] Hachem-Vermette C, Singh K. Mixed-use neighborhoods layout patterns: Impact on solar access and resilience. Sustainable Cities and Society. 2019;51.
- [10] Hong B, Lin BR. Numerical studies of the outdoor wind environment and thermal comfort at pedestrian level in housing blocks with different building layout patterns and trees arrangement (vol 73, pg 18, 2015). Renewable Energy. 2018;126:583-.

- 790 [11] Salvati A, Coch H, Morganti M. Effects of urban compactness on the building energy  
791 performance in Mediterranean climate. *Enrgy Proced.* 2017;122:499-504.
- 792 [12] Mohajeri N, Upadhyay G, Gudmundsson A, Assouline D, Kampf J, Scartezzini JL.  
793 Effects of urban compactness on solar energy potential. *Renewable Energy.* 2016;93:469-  
794 82.
- 795 [13] Morganti M, Salvati A, Coch H, Cecere C. Urban morphology indicators for solar  
796 energy analysis. *Sustainability in Energy and Buildings* 2017. 2017;134:807-14.
- 797 [14] Chen YH, Wu JT, Yu K, Wang DD. Evaluating the impact of the building density and  
798 height on the block surface temperature. *Building and Environment.* 2020;168.
- 799 [15] Hu YF, Dai ZX, Guldman JM. Modeling the impact of 2D/3D urban indicators on  
800 the urban heat island over different seasons: A boosted regression tree approach. *Journal of*  
801 *Environmental Management.* 2020;266.
- 802 [16] Ahmadian E, Sodagar B, Bingham C, Elnokaly A, Mills G. Effect of urban built form  
803 and density on building energy performance in temperate climates. *Energ Buildings.*  
804 2021;236.
- 805 [17] Xia B, Li ZH. Optimized methods for morphological design of mesoscale cities based  
806 on performance analysis: Taking the residential urban blocks as examples. *Sustainable*  
807 *Cities and Society.* 2021;64.
- 808 [18] Heng CK, Malone-Lee LC, Zhang J. Relationship between density, urban form and  
809 environmental performance. *Growing Compact: Routledge;* 2017. p. 297-312.
- 810 [19] Abusaada H, Elshater A. COVID-19 and "the trinity of boredom" in public spaces:  
811 urban form, social distancing and digital transformation. *Archnet-Ijar.* 2022;16:172-83.
- 812 [20] Bahrainy H, Khosravi H. The impact of urban design features and qualities on

813 walkability and health in under-construction environments: The case of Hashtgerd New  
814 Town in Iran. *Cities*. 2013;31:17-28.

815 [21] Zhou WQ, Pickett STA, Cadenasso ML. Shifting concepts of urban spatial  
816 heterogeneity and their implications for sustainability. *Landscape Ecology*. 2017;32:15-30.

817 [22] Cheng V, Steemers K, Montavon M, Compagnon R. Urban Form, Density and Solar  
818 Potential. 2006.

819 [23] Chatzipoulka C, Compagnon R, Nikolopoulou M. Urban geometry and solar  
820 availability on fa ades and ground of real urban forms: using London as a case study. *Sol*  
821 *Energy*. 2016;138:53-66.

822 [24] Lan HF, Gou ZH, Hou CY. Understanding the relationship between urban morphology  
823 and solar potential in mixed-use neighborhoods using machine learning algorithms.  
824 *Sustainable Cities and Society*. 2022;87.

825 [25] Poon KH, Kampf JH, Tay SER, Wong NH, Reindl TG. Parametric study of URBAN  
826 morphology on building solar energy potential in Singapore context. *Urban Climate*.  
827 2020;33.

828 [26] Zhu R, Wong MS, You L, Santi P, Nichol J, Ho HC, et al. The effect of urban  
829 morphology on the solar capacity of three-dimensional cities. *Renewable Energy*.  
830 2020;153:1111-26.

831 [27] Liao W, Hong T, Heo Y. The effect of spatial heterogeneity in urban morphology on  
832 surface urban heat islands. *Energ Buildings*. 2021;244.

833 [28] Yang XY, Li YG. The impact of building density and building height heterogeneity on  
834 average urban albedo and street surface temperature. *Building and Environment*.  
835 2015;90:146-56.

836 [29] Shareef S. The impact of urban morphology and building's height diversity on energy  
837 consumption at urban scale. The case study of Dubai. *Building and Environment*. 2021;194.  
838 [30] Yang H, Wang M, Peng J. Actual Performances of PV Panels in the Local Environment.  
839 2020.  
840 [31] Hong Kong Electrical and Mechanical Services Department. Hong Kong Energy End-  
841 use Data 2022. 2022.  
842 [32] Hong Kong Environment and Ecology Bureau. Hong Kong's Climate Action Plan  
843 2050. 2021.  
844 [33] Coseo P, Larsen L. How factors of land use/land cover, building configuration, and  
845 adjacent heat sources and sinks explain Urban Heat Islands in Chicago. *Landscape and*  
846 *Urban Planning*. 2014;125:117-29.  
847 [34] Mohajeri N, Gudmundsson A, Kunckler T, Upadhyay G, Assouline D, Kampf JH, et  
848 al. A solar-based sustainable urban design: The effects of city-scale street-canyon geometry  
849 on solar access in Geneva, Switzerland. *Applied Energy*. 2019;240:173-90.  
850 [35] Perini K, Magliocco A. Effects of vegetation, urban density, building height, and  
851 atmospheric conditions on local temperatures and thermal comfort. *Urban Forestry &*  
852 *Urban Greening*. 2014;13:495-506.  
853 [36] Vermeulen T, Kämpf JH, Beckers B. Urban form optimization for the energy  
854 performance of buildings using Citysim. EPFL Solar Energy and Building Physics  
855 Laboratory (LESO-PB); 2013.  
856 [37] Lauzet N, Rodler A, Musy M, Azam MH, Guernouti S, Mauree D, et al. How building  
857 energy models take the local climate into account in an urban context - A review.  
858 *Renewable & Sustainable Energy Reviews*. 2019;116.



859 [38] Natanian J, Aleksandrowicz O, Auer T. A parametric approach to optimizing urban  
860 form, energy balance and environmental quality: The case of Mediterranean districts.  
861 Applied Energy. 2019;254.

862 [39] Huo TF, Xu LB, Liu BS, Cai WG, Feng W. China's commercial building carbon  
863 emissions toward 2060: An integrated dynamic emission assessment model. Applied  
864 Energy. 2022;325.

865 [40] Nault É. Solar potential in early neighborhood designa decision-support workflow  
866 based on predictive models: EPFL; 2016.

867 [41] Ko YK. Urban Form and Residential Energy Use: A Review of Design Principles and  
868 Research Findings. Journal of Planning Literature. 2013;28:327-51.

869 [42] Huo TF, Cao RJ, Xia NN, Hu X, Cai WG, Liu BS. Spatial correlation network structure  
870 of China's building carbon emissions and its driving factors: A social network analysis  
871 method. Journal of Environmental Management. 2022;320.

872 [43] Wang X, Li HD, Sodoudi S. The effectiveness of cool and green roofs in mitigating  
873 urban heat island and improving human thermal comfort. Building and Environment.  
874 2022;217.

875 [44] Dai HK, Chen C. Air infiltration rates in residential units of a public housing estate in  
876 Hong Kong. Building and Environment. 2022;219:109211.

877 [45] Hong Kong Buildings Department. Guidelines on Design and Construction  
878 Requirements for Energy Efficiency of Residential Buildings. 2014.

879 [46] Fung SF, Lu L. Thermal performance analysis on different types of glazing of public  
880 rental housing in Hong Kong. Procedia Engineer. 2017;205:794-801.

881 [47] Kwok YT, Lau K, Ng E. The influence of building envelope design on the thermal

882 comfort of high-rise residential buildings in Hong Kong2018.

883 [48] BEAM Society Limited. BEAM Plus for New Buildings Version 1.2. 2012.

884 [49] HK Electric Investments. HKEI Sustainability Report 2021. 2021.

885 [50] CLP Power Hong Kong Limited. CLP 2021 Sustainability Report. 2021.

886 [51] The Hong Kong and China Gas Company Limited. Towngas Environmental, Social

887 and Governance Report 2021. 2021.

888